FTIR and photoluminescence of annealed silicon rich oxide films

J. A. Luna-López*, J. Carrillo-López
CIDS-ICUAP, Benemérita Universidad de Puebla
Ed. 136, Col, San Manuel. Puebla, Pue. México 72570

M. Aceves-Mijares, A. Morales-Sánchez
Instituto Nacional de Astrofísica Óptica y Electrónica
Apdo. 51 Puebla, Pue. 72000, México

C. Falcony
Departamento Física, CINVESTAV
Apdo. 17-740 México D.F., México 07000
(Recibido: 16 de noviembre de 2008; Aceptado: 30 de enero de 2009)

In order to have optoelectronic function integrated in a single chip, it is very important to obtain a silicon compatible material with an optimal Photoluminescence (PL) response. The Silicon Rich Oxide (SRO) has shown intense PL and is also compatible with silicon technology.
In this work, the composition and optical properties of the SRO films are studied using null Ellipsometry, Fourier Transformed Infrared spectroscopy (FTIR), and Photoluminescence (PL). The SRO films were annealed at high temperature during different times. The IR absorption spectra show the presence of three characteristics Si-O-Si vibrations modes in SiO_2. However, changes in their intensity and position were observed when annealing time and silicon excess were varied. These changes are directly related with structural variation in the SRO films. PL spectra show a considerable emission in the range 650 to 850 nm that varies with different thermal treatment times.

Keywords: Silicon Rich Oxide (SRO); Silicon nanoparticles; Refractive index; Photoluminescence; FTIR

1. Introduction

Since the discovery of light emission from porous silicon [1], an intense investigation of materials compatible with silicon technology and with excellent optical emission properties has been under development. Therefore, a great variety of materials with these characteristics has been studied [2-3]. One of these materials is the Silicon Rich Oxide (SRO) [4].

The optical characteristics of SRO can be varied with the excess silicon in the films, making SRO attractive to fabricate optoelectronic devices. For example refractive index varies from 1.45 to 1.94 when the silicon excess varies, and similarly photoluminescence spectra are highly dependent on silicon excess. These characteristics have given place to various types of applications as wave guides, no volatile memories, peaks suppressers, light radiation and detection devices [5-7].

The SRO can be obtained through several techniques. One of the most useful is Low Pressure Chemical Vapour Deposition (LPCVD). This technique allows obtaining films with variable silicon excess just varying the flow ratio (Ro) of silane (SiH_4) and nitrous oxide (N_2O) during the deposition:

$$Ro = [N_2O]/[SiH_4].$$

In this work, refractive index, FTIR and PL characteristics of SRO films prepared by LPCVD are presented and compared ith SiO_2. The influence of the Ro (silicon excess) and annealing temperature on these films are investigated. The optical and compositional characteristics to understand the possible emission mechanism of the SRO films are studied.

2. Experiment

SRO films were deposited in a horizontal low-pressure CVD hot-wall reactor using SiH_4 and N_2O as the reactant gases at 700 ºC. The flow ratio Ro of SiH_4 and N_2O was used to control the amount of excess silicon in the SRO films to obtain Ro = 10, 20 and 30. The total gas pressure was varied from 1.64 to 1.94 Torr for the different Ro´s. SRO thickness was ~ 500 nm. Subsequently the films were densified in N_2 during 30 minutes at 1000 °C, and then annealed. The annealing was at 1100 ºC in a nitrogen, and the duration was 30, 60 and 180 minutes. SiO_2 films were thermally grown in a furnace at 1000 ºC with a gas mixture of O_2 and TCE (Trichloroethylene). SiO_2 thickness was ~ 120 nm.

The refractive index and thickness were measured with a null Ellipsometer Gaertner L117 with a laser of He-Ne (632.8 nm). FTIR Spectroscopy measurements were done using a Brucker system model vector 22. PL response was measured at room temperature using a Perkin-Elmer spectrometer model LS-50B with a pulsed xenon source whose detector has a multiplier tube. The samples were

*jluna@inaoep.mx

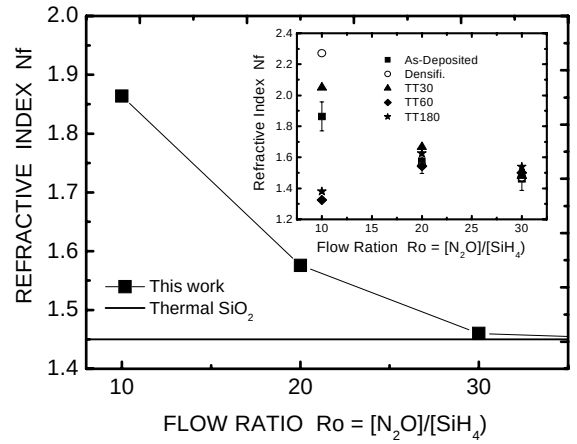

Figure 1. Refractive index as a function of Ro for as-deposited films, a comparison with thermal SiO_2 is done. The inset shows the Refractive index as a function of Ro for different annealing times.

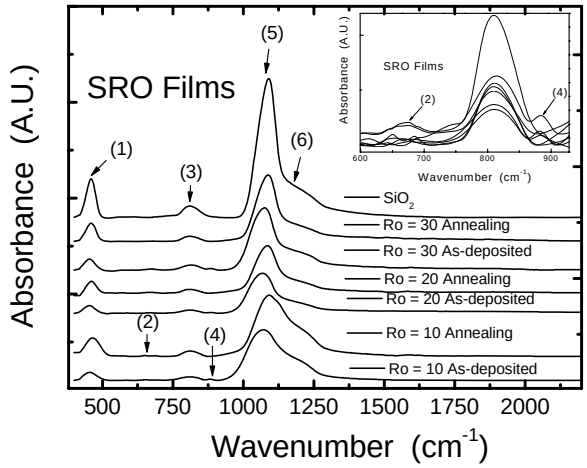

Figure 2. FTIR Absorption Spectra of the SRO films of Ro = 10, 20 and 30 after different annealing, and absorption spectra of thermal SiO_2. The capital letters (R), (B) and (S) mean Rocking, Bending and Stretching vibration modes.

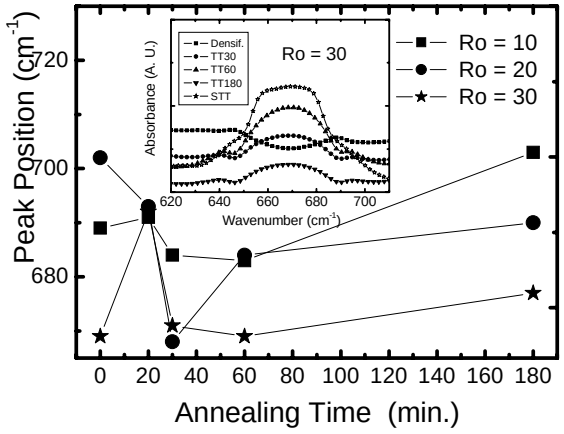

Figure 3. Peak position of the vibration modes at 660-680 cm^{-1} as a function of the annealing time for SRO films, the inset shows the absorption peak for Ro = 30.

excited using 250 nm and PL response was recorded between 400 and 900 nm with a 2.5 nm resolution.

3. Results

The refractive index of the SRO films as a function of Ro is shown in Fig. 1; the refractive index of the thermal SiO_2 film is also shown. Inset of Fig. 1 shows the behaviour of the refractive index at different times of thermal treatment (TT). For Ro = 10, the refractive index varies with the time of annealing. An increase is observed in the refractive index after the treatment at 1000 °C then it decreases with annealing time at 1100 °C, the variation is noticeable. However, for Ro = 20 and 30 similar behaviour is observed, but the variation is within the error bars approximately. The refractive index of SRO films also augments with the excess of silicon, and with the thermal treatment time.

The FTIR absorption spectra of as-deposited and annealed SRO films with different silicon excess are shown in Fig. 2; the spectrum of thermal SiO_2 is also shown as a reference. These spectra show the absorption peaks associated with stretching (1084 cm^{-1}), bending (812 cm^{-1}) and rocking (458 cm^{-1}) vibration modes of the Si-O-Si bonds in SiO_2 [7-9]. The position of the stretching absorption peak changes with the Ro value and with thermal treatments.

Table 1 show the peaks position of the Si-O, Si-Si and Si_2O_3 bonds. Their peak position moves toward a higher wavenumber with annealing. On the other hand, the out of phase stretching peak position does not show a big change. Then, the peak position (6) for Ro = 10 is almost constant with different Thermal Treatments.

Figure 3 shows the behaviour of the weak absorption peak at 670-690 cm^{-1}. This peak is present in the IR spectra of all Ro's; the inset shows the same peak for Ro = 30.

Figure 4 shows the PL response from SRO films corresponding to Ro= 10, 20 and 30, after annealing. Emission in the range of 600 to 900 nm, with an intense peak around 725 nm (1.7 eV) is observed.

Fig. 4 a) shows that for Ro = 10, the PL has the weakest intensity compared with Ro =20 and 30. PL bands increase with annealing time.

4. Analysis and Discussion

The refractive indexes of the SRO increase with the increase of excess Si. As Ro increases the index tends toward that of SiO_2, and on the other way towards that of Si. Then, the inclusion of Si in these films is evident. For Ro = 10, after annealing, the refractive index varies without a clear tendency but the change is big. In Ro = 20 and 30 the tendency is more clear. In atomic force microscope, AFM, studies of this material was observed that for SRO annealed at 1100 °C the surface was rough, and the roughness reduces as Ro increases. Being SRO_{10} the bumpiest compared with $SRO_{20, 30}$, with hills as high as 24 nm for Ro = 10, and for Ro =30 the hills are five times

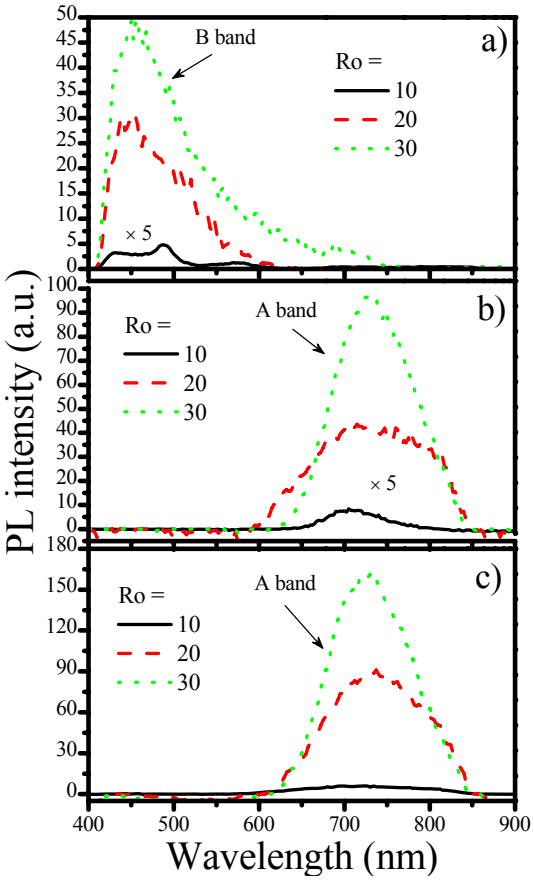

Figure 4. PL spectra of SRO with Ro = 10, 20 and 30 and a) as-deposited, b) densified at 1000 ºC for 30 min, and c) thermally annealed at 1100 ºC.

smaller [10]. The high roughness of Ro = 10 is probably the cause of the index variation without a clear tendency, and the roughness could be due to the big nanocrystals embedded in the SRO.

Results of infrared spectroscopy are shown in Table 1, where the absorption peaks, their identifications and references are recorded. In the as-deposited films the frequency of stretching vibration peak (peak No.5) increases with Ro; and the shoulder (peak No.6) is assigned to the asymmetric stretching vibration mode of Si-O-Si bond and also shifts to higher frequency.

Table 1 shows that the position of peak (5) changes after thermal treatments. This peak moves toward a higher frequency approaching to that of the thermal silicon dioxide. We have also calculated the ratio of absorption strengths between peaks (6) and (5). The ratio for SiO_2 is 0.43, while that for SRO increases from 0.5 to 0.95 when Ro changes from 30 to 10, both in the in the as-deposited and annealed state [9, 11]. Thermal annealing did not change the ratio of absorption strengths between peaks (6) and (5) for each Ro; this indicates that thermal annealing did not change the silicon content in SRO [9, 12]. The only change produced by thermal annealing is with regard to the microstructure of the films, the radiative defects can be activated with the heating processes. Furthermore, after annealing, the full width half maximum (FWHM) of the peak (5) reduces indicating that SRO network becomes more ordered. This result also agrees with the refractive index, which indicates the densification of the films [13].

The position of peak (5) of the annealed samples does not depend on silicon excess, as shown in Table 1. This is an evidence that the annealed SRO films do not have large content of sub-stoichiometric SiO_x ($x<2$) phase although it really does in the as-deposited state. If the annealed SRO films contained large amount of substoichiometric oxide phase, the peak (5) should shift towards lower frequency; and this shift should also increase with the Si excess. In other words, this result suggests that phase-separation into stoichiometric SiO_2 and Si nanoparticles (Si-nps) occurred during the thermal annealing process, regardless the Si excess.

An absorption peak at ~680 cm^{-1} in the IR spectra of both as-deposited and annealed films is presented, as shown in the inset of Fig. 3. This peak has been assigned to neutral oxygen vacancies (possibly NOV, E' centres, and NBOHC), which is described as ≡Si-Si≡ or similar compounds in β-cristobalite, where the cristobalite is a polymorph of the SiO_2 [14]. Other authors [15, 16] suggested that the peaks at 660─690 cm^{-1} are an indicative of a great density of Si-Si bonds. In our samples, this peak is still present after annealing, indicating that it is probably associated with Si-nps. In Annealed samples reduces the content of sub-stoichiometric oxide, implying that there is a restructuration of the different phases.

Also, it is shown an absorption peak at 885 cm^{-1}. This peak is associated with sub-oxidized silicon species (oxygen interstitials) and is due to the structural combination of Si_2O_3, [14, 17], which disappears after thermal treatments. This is another evidence of phase-separation during the thermal annealing.

PL bands around 725 nm often appear in annealed SRO films. However, their characteristics and behaviour always show some differences which are associated with the deposition technique and the experimental conditions used. In general, the 725 nm band presents a similar behaviour to that one reported for others authors in similar materials [15, 16]. Its origin is usually ascribed to quantum dots, interface defects of the Si/SiO_2 interface and defects associated with oxygen in the film. It is possible that before applying the thermal treatment these defects were in the film as neutral charged oxygen vacancies (NOV) (Si-Si bonds), nonbridging oxygen hole center (NBOHC), positively charged oxygen vacancies (E' centres), interstitial oxygen molecules and peroxide radicals [3, 14-17]. Some of the radiative defects such as NOV (Si-Si bonds), and NBOHC can be activated with the annealing processes, which can form Si-nps or E' centres. Therefore, the increase of the PL with the annealing time is due to the activation of the radiative defects. In this study the 725 nm PL band has been correlated with silicon excess in the film as NOV as Si-nps and defects [11, 18], and has strong correlation with annealing temperature and time. This Band is well defined only if the film has been thermally treated at temperature

Table 1. FTIR vibrations modes in the as-deposited and after annealed SRO films.

Vibration type	**Reference**	**SiO_2**	**Wavenumber** (SRO) (cm^{-1})					
			As-deposited			Annealing		
			10	20	30	10	20	30
(1) Si-O rocking	7, 9, 10	458	450	453	450	457	458	458
(2) Si-Si (Oxygen's Vacancies)	12, 13, 14	-	689	702	669	703	690	677
(3) Si-O bending	7, 9, 10	812	815	805	811	810	811	812
(4) Si_2O_3	15, 16	-	883	885	883	-	-	-
(5) Si-O stretching on phase	7, 9, 10	1082	1061	1063	1068	1088	1080	1082
(6) Si-O stretching out of phase	7, 9, 10	1177	1147	1178	1185	1149	1145	1160

higher than 1000°C in N_2 atmosphere and annealing time is higher than 30 minutes. If the film has been submitted to thermal treatment at 1100 °C the 725 nm band reaches its maximum PL emission.

5. Conclusions

SRO films were deposited on silicon substrates by LPCVD with different silicon excess (Ro) and different thermal annealing was applied. The annealing was done in nitrogen at 1100°C and during different times. The structural and optical properties of silicon-rich oxide were studied. The effect of the different thermal annealing time on the properties of SRO was investigated.

Refractive index, FTIR spectroscopy and Photoluminescence characteristic of the films were studied as a function of the flow ratio Ro and thermal treatment time. Refractive index of the SRO films increases with the excess Si.

The variation of the IR spectra shown the effect of the Ro`s (silicon excess) and the thermal treatment time on the SRO films. The shifts of the stretching vibration mode peaks of the Si-O-Si bonds are indicative of the change of the stoichiometry of SRO films. In SRO films with annealing, the stretching peak position is shifted towards higher frequency. This is ascribed to a phase separation in the SRO films.

The FTIR peak observed on the 650-690 cm^{-1} range is caused by vibrations associated with defects as neutral vacancies of oxygen ≡Si-Si≡, or similar composites. Si_2O_3 compounds were related to a peak observed at 882-885 cm^{-1}, which disappears with the thermal annealing. This is another evidence of phase-separation during the thermal annealing.

The as-deposited SRO films contain sub-stoichiometric oxide and Si-nps. IR measurements evidenced that thermal annealing results in a phase separation, and then Si-nps embedded in stoichiometric oxide matrix are produced.

Juárez and Netzhualcoyotl Carlos for their help in the preparation of the samples.

References

[1]Canham L.T., Appl. Phys. Lett. 57, 1046(1990).
[2]Song H.Z. and Bao X.M., Phys. Rev. B **55**, 6988(1997).
[3]Inokuma T., Wakayama Y., Muramoto T., Auki R., Muramoto Y., and Hasegawa S., J. Appl. Phys. **83**, 2228(1998).
[4]Wisken F., Amans D., /Ledoux G., Hofmeister H., Cichos F., and Martin J., New J. Phys. **5**, 10(2003).
[5]M. Aceves, A. Malik, and R. Murphy, In: Sensors and Chemometrics, eds: Maria Teresa Ramirez-Silva, (Research Signpost, ISBN: 81-7736-067-1, 2001) p.1-25.
[6]D. J. DiMaria, D. W. Dong, F. L. Pesavento, J. Appl. Phys., **55**, 3000(1984).
[7]F. Ay, A. Aydinly, Optical Materials **26**, 33(2004).
[8]M. Aceves, D. Berman, J. Carranza, L. Berriel, C. Domínguez, Nanotechnology, Anaheim, California USA (2005).
[9]P. G. Pai, S. S. Chao, Y. Takagi, and G. Lucovsky, J. Vac. Sci. Technol., A **4**, 689 (1986).
[10] Pereyra, Alayo, Thin solid Films **402**, 161(2002).
[11] J. A. Luna-Lopez, M. Aceves-Mijares, O. Malik, Z. Yu, A. Morales, C. Dominguez and J. Rickards, Revista Mexicana de Física, **53**, 293 (2007).
[12] Zhenrui Yu, Mariano Aceves, A. Luna López, Enrique Quiroga, R. Lopez-Estopier, Focus on Nanomaterials Research. Cap. 9. Editors: Nova Science Publishers, (2006).
[13] A. Luna-Lopez, M. Aceves, O. Malik, Proceedings of the 2nd ICEEE-CIE 2005, IEEE catalog Num. 05EX1097, 435 (2005).
[14] Tomonari Morioka, Seiji Kimura, Noritoshi Tsuda, Chihiro Taito, Yoshio Saito and Chiyoe Koike, Mon. Not. R. Astron. Soc. **299**, 78 (1998).
[15] Inokuma T., Kurata Y. and Hasewaga S., Journal of Electroluminescence **80**, 247 (1999).
[16] Bairle R. J., Caldas M. J., Molinari E., Ossicini S., Solid State Communications **102**, 545 (1997).
[17] Minoru Nakamura, Yasuhiro Mochizuki, and Katsuhisa Usami, Solid State Communications **50**, 1079 (1984).
[18] Z. Yu, M. Aceves-Mijares, A. Luna-Lopez, jinhui Du and Dongcai Bian, Nanotechnology **17**, 4962 (2006).